NeuroImage: Clinical 20 (2018) 357–364

Contents lists available at ScienceDirect

NeuroImage: Clinical

journal homepage: www.elsevier.com/locate/ynicl

Integrated imaging of [^{11}C]-PBR28 PET, MR diffusion and magnetic resonance spectroscopy ^{1}H-MRS in amyotrophic lateral sclerosis

Eva-Maria Ratai[a,b,1], Mohamad J. Alshikho[a,c,1], Nicole R. Zürcher[a], Marco L. Loggia[a], Catherine L. Cebulla[c], Paul Cernasov[c], Beverly Reynolds[c], Jennifer Fish[c], Raghav Seth[a], Suma Babu[c], Sabrina Paganoni[c], Jacob M. Hooker[a], Nazem Atassi[c,*]

[a] A. A. Martinos Center for Biomedical Imaging, Department of Radiology, Massachusetts General Hospital, Harvard Medical School, Charlestown, MA, USA
[b] Department of Radiology, Neuroradiology Division, Massachusetts General Hospital, Harvard Medical School, Boston, MA, USA
[c] Neurological Clinical Research Institute (NCRI), Department of Neurology, Massachusetts General Hospital, Harvard Medical School, Boston, MA, USA

ARTICLE INFO

Keywords:
^{1}H-MRS
PET
Glial activation
Amyotrophic lateral sclerosis
[^{11}C]-PBR28
DTI

ABSTRACT

Objective: To determine the relationship between brain tissue metabolites measured by *in vivo* magnetic resonance spectroscopy (^{1}H-MRS), and glial activation assessed with [^{11}C]-PBR28 uptake in people with amyotrophic lateral sclerosis (ALS).

Methods: Forty ALS participants were evaluated clinically using the revised ALS functional rating scale (ALSFRS-R) and upper motor neuron burden (UMNB). All participants underwent simultaneous brain [^{11}C]-PBR28 PET and MR imaging including diffusion tensor imaging to acquire fractional anisotropy (FA). [^{11}C]-PBR28 uptake was measured as standardized uptake values normalized by whole brain mean (SUVR). ^{1}H-MRS metabolite ratios (myo-inositol/creatine, mI/Cr; *N*-acetylaspartate/creatine, NAA/Cr) were measured within the precentral gyri and brain stem (regions known to be involved in ALS pathophysiology), and precuneus (which served as a control region). Whole brain voxel-wise correlation analyses were employed to identify brain regions exhibiting an association between metabolites within the VOIs and [^{11}C]-PBR28 uptake.

Results: In the precentral gyri, [^{11}C]-PBR28 uptake correlated positively with mI/Cr and negatively with NAA/Cr. The same correlations were not statistically significant in the brain stem, or in the control precuneus region. Whole brain voxel-wise correlation analyses between the estimated brain metabolites within the VOIs and SUVR were highly correlated in the precentral gyri. Decreased FA values in the precentral gyri were correlated with reduced NAA/Cr and elevated mI/Cr. Higher UMNB was correlated with increased [^{11}C]-PBR28 uptake and mI/Cr, and decreased NAA/Cr. ALSFRS-R total score correlated positively with NAA/Cr and negatively with mI/Cr.

Conclusion: Integrated PET-MR and ^{1}H-MRS imaging demonstrates associations between markers for neuronal integrity and neuroinflammation and may provide valuable insights into disease mechanisms in ALS.

1. Introduction

Genetic and postmortem human brain pathology studies implicate glial activation and neuroinflammation in ALS (Alexianu et al., 2001; Butovsky et al., 2012; Boillee et al., 2006; Cady et al., 2014; Brettschneider et al., 2012). In contrast to postmortem pathological studies, molecular neuroimaging provides an opportunity to study and track ALS mechanisms, *in vivo,* and to potentially measure the biological

Abbreviations: ^{1}H-MRS, proton magnetic resonance spectroscopy; ALS, amyotrophic lateral sclerosis; ALSFRS-R, revised ALS functional rating scale; Cr, creatine; DTI, diffusion tensor imaging; FA, fractional anisotropy; mI, myo-inositol; MEMPRAGE, multi-echo magnetization prepared rapid acquisition gradient echo; NAA, *N*-acetylaspartate; PRESS, point-resolved spectroscopy; PBR, peripheral benzodiazepine receptor.; SUV, standardized uptake value; SUVR, standardized uptake value normalized to whole brain mean; TSPO, translocator protein; UMNB, upper motor neuron burden; VOI, volume of interest

* Corresponding author at: Neurological Clinical Research Institute (NCRI), Massachusetts General Hospital, 165 Cambridge Street, Suite 656, Boston, 02114, MA, USA.

E-mail addresses: eratai@mgh.harvard.edu (E.-M. Ratai), malshikho@mgh.harvard.edu (M.J. Alshikho), zurcher@nmr.mgh.harvard.edu (N.R. Zürcher), marco@nmr.mgh.harvard.edu (M.L. Loggia), ccebulla@mgh.harvard.edu (C.L. Cebulla), paul.cernasov@unc.edu (P. Cernasov), bvreynolds@mgh.harvard.edu (B. Reynolds), sbabu@mgh.harvard.edu (S. Babu), spaganoni@mgh.harvard.edu (S. Paganoni), hooker@nmr.mgh.harvard.edu (J.M. Hooker), natassi@mgh.harvard.edu (N. Atassi).

[1] Contributed equally.

https://doi.org/10.1016/j.nicl.2018.08.007
Received 15 March 2018; Received in revised form 3 August 2018; Accepted 5 August 2018
Available online 09 August 2018

effects of experimental treatments (Jucaite et al., 2015).

Upon activation, microglia and astrocytes undergo increased expression of the 18 kDa translocator protein (TSPO), previously known as the peripheral benzodiazepine receptor (PBR) (Rupprecht et al., 2010). [^{11}C]-PBR28 is a second-generation positron emission tomography (PET) radiotracer for TSPO (Lavisse et al., 2012; Brown et al., 2007; Briard et al., 2008), and as such is used to image neuroinflammation *in vivo* (Albrecht et al., 2016). [^{11}C]-PBR28 was developed to overcome challenges associated with the first-generation TSPO radioligands. [^{11}C]-PBR28 was shown to exhibit 80 times more specific binding compared to the first generation radioligand [^{11}C] -(*R*)-PK11195 in non-human primates (Sridharan et al., 2017; Kreisl et al., 2010).

Glial activation measured by [^{11}C]-PBR28 PET is increased in the precentral gyri in patients with ALS and other motor neuron diseases (Paganoni et al., 2018; Zurcher et al., 2015), and this increase co-localizes with microstructural alterations measured by changes in fractional anisotropy (FA) and cortical thickness (Alshikho et al., 2016). Here, we employ a multimodal neuroimaging approach using [^{11}C]-PBR28 PET, magnetic resonance spectroscopy (^{1}H-MRS), and diffusion tensor imaging (DTI) to evaluate the relationship between glial activation and brain structural integrity, as well as the clinical outcome measures in ALS patients.

N-acetylaspartate (NAA) and myo-inositol (mI) are brain metabolites that can be measured by ^{1}H-MRS and are thought to serve as markers of neuronal/axonal integrity and neuroinflammation/gliosis, respectively (Moffett et al., 2007; Brand et al., 1997).

The relationship between molecular measurements derived from PET modalities and ^{1}H-MRS brain tissue metabolites has never been tested in patients with ALS. This molecular multimodal imaging approach may provide invaluable insights into disease mechanisms and could guide future therapeutic interventions.

2. Materials and methods

2.1. Standard protocol approvals, registrations, and patient consents

This study was approved by the Partners institutional review board (IRB) and the radioactive drug research committee (RDRC) at Massachusetts General Hospital (MGH), Boston, MA. All participants provided written informed consent for study participation according to the declaration of Helsinki.

2.2. Study participants and clinical assessments

Between March 2014 and December 2016, sixty-three individuals were genotyped for TSPO Ala147Thr polymorphism, which predicts [^{11}C]-PBR28 binding affinity (Guo et al., 2014; Owen et al., 2012), and five low binders (7.8%) were excluded during the screening phase of the study. Forty ALS participants, high or mixed TSPO binders, who successfully completed PET-MR brain imaging and fulfilling the revised El Escorial diagnostic criteria for possible, probable, lab-supported probable, or definite ALS, were included in the study (Brooks et al., 2000). The clinical assessment of ALS participants included the revised ALS functional rating scale (ALSFRS-R) (Cedarbaum et al., 1999), and the upper motor neuron burden scale (UMNB) (Zurcher et al., 2015). Participants were excluded if they had any contraindication to undergo MR imaging ($n = 3$), or any current use of steroids, immunosuppressants ($n = 2$), benzodiazepines or non-steroidal anti-inflammatory medications. Patients with frontotemporal dementia, chronic inflammatory conditions, or recent history of an active infection were also excluded.

2.3. PET-MR data acquisition

[^{11}C]-PBR28 was produced in-house as previously described (Imaizumi et al., 2007). At injection time, the mean [SD] bolus injection of [^{11}C]-PBR28 was 465.31 [77.29] MBq. All imaging studies were performed at a single site using a Siemens 3 T Magnetom Tim Trio scanner (Siemens Erlangen, Germany) equipped with an 8-channel head coil, and a head-only PET camera to simultaneously acquire PET-MR images. The PET scanner consisted of dedicated brain avalanche photodiode based PET scanner that operated in the bore of a 3 T whole-body MR scanner. The spatial resolution in the center field-of-view was < 3 mm. Additional information about the PET system was described in detail in previous publications (Catana et al., 2010; Kolb et al., 2012).

MR data acquisition included:

1) T1-weighted 3D multi-echo magnetization prepared rapid acquisition gradient echo (MEMPRAGE) for the purposes of anatomical localization, spatial normalization as well as attenuation correction for the PET data (Izquierdo-Garcia et al., 2014).
2) Diffusion tensor imaging (DTI) data were acquired using a single-shot, spin-echo and echo-planar imaging (EPI) sequence ($b = 3000$ s/mm^2) with twice refocused spin echo diffusion preparation (Q-ball imaging). Each set of raw diffusion data included sixty diffusion directions and eight low-b images.
3) Four ^{1}H-MRS volumes of interest (VOIs) of 8 cm^3 were placed based on the MEMPRAGE images in the left and right precentral gyri including the underlying white matter, in the brain stem as regions of interest, and in the precuneus as a control region, as the latter is not known to be implicated in ALS pathophysiology. We placed one voxel in the precuneus as a bilateral structure because it is a medial structure, and the left and right precuneus are close to each other. Since the precuneus is not known to be involved in ALS, we didn't need to make a distinction between the left and right precuneus, and we used it as one control region. These placements of the VOIs were done manually by an experienced neurologist as well as a spectroscopist. Prior to data acquisition, the ^{1}H-MRS VOIs underwent an automatic shim routine based on gradient double acquisition (GRE-shim) using first and second order shims followed by first order manual shimming. A point-resolved spectroscopy (PRESS) sequence was used to measure brain metabolites. The acquisition parameters for the MR data are summarized in Supplementary Table 1.

2.4. Data processing

The PET images were acquired 60–90 min post radiotracer injection, and [^{11}C]-PBR28 uptake was quantified as standardized uptake value ratio (SUVR) normalized by whole brain mean (Zurcher et al., 2015; Alshikho et al., 2016). Further details are summarized in prior publication (Izquierdo-Garcia et al., 2014). The preprocessing steps of the raw diffusion data were performed using FMRIB Software Library FSL (v5.0.9, https://fsl.fmrib.ox.ac.uk/fsl/fslwiki/). Diffusion data were examined carefully for motion artifacts, and corrected for eddy current-induced distortions and head motion (Andersson and Sotiropoulos, 2016).

After ^{1}H MRS acquisition, data were exported as binary remote data access (RDA) files which include information about the geometrical characteristics of the VOIs (*i.e.* location, dimensionality, and its rotation in space) in the native space of participants. This procedure allowed the creation of 3D masks representing the exact location and orientation of the ^{1}H-MRS voxel placement using the “mri_volsynth” tool in Freesurfer (v6·0, https://surfer.nmr.mgh.harvard.edu/), which were then used to quantify all the other PET-MR measurements within the VOIs. Tools in Freesurfer were used to compute PET-MR measures within the VOIs.

LCModel (v6.3) was used to quantify myo-inositol (mI), creatine (Cr), and *N*-acetylaspartate (NAA), within the VOIs. The analysis was performed within the chemical shift range (0.5–4 ppm). The concentrations of mI and NAA were normalized by Cr concentration and expressed as ratios of mI/Cr and NAA/Cr as commonly done (Pohl

et al., 2001; Kenn et al., 2001; Kalra et al., 2006). Eddy current correction was applied on ^{1}H-MRS data using LC Model.

Finally, technical difficulties (*i.e.* low quality of data or scanning time limitations) during MR spectroscopy, DTI and PET scanning sessions led to excluding thirteen imaging datasets form the analyses. Specifically, PET data were not available for three subjects due to interruptions during PET data acquisition (*i.e.* data were not available for 60-90 min post radiotracer injection). ^{1}H-MRS data were not available for three subjects due to scanning time limitations and two ^{1}H-MRS subjects were excluded due to low quality of the acquired data represented by low signal to noise ratio or chemical shifts. Five diffusion scans were excluded due to motion artifacts.

2.5. Statistical analyses

Pearson correlation analyses were conducted within the four ^{1}H-MRS VOIs to study the relationship between ^{1}H-MRS metabolite concentrations (mI/Cr, NAA/Cr), [^{11}C]-PBR28 uptake measured by mean SUVR, diffusion fractional anisotropy (FA), and the clinical measures including UMNB and ALSFRS-R. To reduce the impact of potential outliers on the correlations, all Pearson correlation analyses were followed by a robust regression fit based on the Huber M-estimation method (Yeap and Davidian, 2001). All the statistical analyses were carried out using JMP pro 13.0 (SAS Institute Inc., Cary, NC, 1989–2014).

In addition, separate whole-brain voxel-wise correlation analyses were employed to identify brain regions exhibiting an association between [^{11}C]-PBR28 uptake and ^{1}H-MRS metabolites extracted from the left and right VOIs. These analyses were performed to test the spatial specificity and colocalization of the association between motor cortex metabolites and [^{11}C]-PBR28 uptake within each voxel in the brain. Non-parametric permutation inference (Winkler et al., 2014) (n = 5000 permutations) and general linear model (GLM) were employed. Threshold free cluster enhancement (TFCE) method (Smith and Nichols, 2009) was applied, and the p values were family-wise error corrected (FWE) for multiple comparisons at an alpha value of 0.05. Sex and [^{11}C]-PBR28 binding affinity were included covariates in the design matrix. In separate analyses, the ratios between the gray and white matter volumes within the left and right VOIs were measured and included as covariates in the GLM.

3. Results

Forty ALS participants were included in this study. There were 17 (42.5%) females and the mean age was (54 ± 10) years. Detailed demographics and clinical data are summarized in Table 1.

Higher levels of mI/Cr were associated with increased [^{11}C]-PBR28 uptake in the left (Fig. 1A; r = + 0.36; p = 0.011), and right (Fig. 1C; r = + 0.49; p = 0.002) precentral gyri. Whole brain voxel-wise correlation analyses confirmed the results and showed significant positive correlation ($P_{FWE} < 0.05$) between mI/Cr and [^{11}C]-PBR28 uptake in the motor and premotor regions, as well as the underlying corticospinal tracts (Fig. 1B, D; $P_{FWE} < 0.05$).

Decreased NAA/Cr was associated with increased [^{11}C]-PBR28 uptake in the left (Fig. 2A; r = - 0.52; p = 0.0006), and right (Fig. 2C; r = - 0.61; $p < 0.0001$) precentral gyri. The results were confirmed by whole brain voxel-wise correlation analyses which revealed significant negative correlation ($P_{FWE} < 0.05$) between NAA/Cr and [^{11}C]-PBR28 uptake in the precentral gyri (Fig. 2B, D; $P_{FWE} < 0.05$).

Including the ratios of the gray and white mater volumes in the left and right VOIs as covariate in the relevant whole brain voxel-wise correlation analyses did not change the results (all analyses conducted with a statistical threshold of $P_{FWE} < 0.05$).

There were significant positive correlations between NAA/Cr and FA in the precentral gyri (Left: r = + 0.50; p = 0.010; Right: r = + 0.62; p = 0.0004) (Fig. 3A, B), and significant negative correlations between mI/Cr and FA in the precentral gyri (Left: r = - 0.36; p = 0.025; Right: r = - 0.50; p = 0.0022) (Fig. 3C, D).

Table 1
Participant Characteristics and clinical assessments[a].

Characteristics	ALS (n = 40)
Age, mean (SD), y	54 (10)
Women	17 (42.5)
Ethnicity	
Not Hispanic/Latino	38 (95)
Hispanic/Latino	1 (2.5)
Unknown	1 (2.5)
Race	
Black	1 (2.5)
White	39 (97.5)
Site of disease onset	
Limb	30 (75)
Bulbar	10 (25)
[^{11}C]-PBR genotype	
ALA/ALA (High)	21 (52.5)
ALA/THR (Mixed)	19 (47.5)
Disease Duration, mean (SD), m	26 (18)
Rate of disease progression (Points/m)	0.67 (0.43)
ALSFRS-R, mean (SD)	37 (6)
UMNB, mean (SD)	27 (5)
Vital capacity, mean (SD)	81.09 (23.4)

[a]Data are reported as No. (%) unless otherwise indicated.
Abbreviations: ALS, amyotrophic lateral sclerosis; ALSFRS-R, revised Amyotrophic Lateral Sclerosis Functional Rating Scale; UMNB, upper motor neuron burden; ALA, alanine; THR, threonine

No significant correlations were found between [^{11}C]-PBR28 uptake and any of these metabolite ratios in the brain stem or in the precuneus control region (Supplementary Table 2).

Lower levels of NAA/Cr were associated with higher UMNB (Left: r = −0.49; P = 0.0023; Right: r = −0.53; p = 0.0036) (Fig. 4A, B) and higher levels of mI/Cr were associated with higher UMNB (Left: r = +0.40; p = 0.009; Right: r = +0.38; p = 0.010) (Fig. 4C, D).

ALSFRS-R and NAA/Cr were positively correlated in the right precentral gyrus (r = +0.54; p = 0.047) but not the left (r = +0.21; p = 0.19) (Supplementary Fig. 1A, B). ALSFRS-R and mI/Cr were negatively correlated in the right precentral gyrus (r = −0.66; p = 0.049) but not the left (r = −0.1; p = 0.54) (Supplementary Fig. 1C, D).

[^{11}C]-PBR28 uptake correlated positively with the UMNB in the right (r = +0.54; $p < 0.0001$), and left precentral gyri (r = +0.53; $p < 0.0001$) (Supplementary Fig. 2A, B). [^{11}C]-PBR28 uptake did not correlate with ALSFRS-R total score, nor with ALSFRS-R subtotal scores (*i.e.* fine motor, gross motor, bulbar and respiratory).

The results of all Pearson correlation analyses are listed in Supplementary Table 2.

4. Discussion

Prior studies have shown that patients with ALS have increased [^{11}C]-PBR28 uptake in the motor cortices (Zurcher et al., 2015) that correlates and co-localizes with structural MRI changes (Alshikho et al., 2016). This study implements multimodal molecular neuroimaging tools to evaluate the relationship between ^{1}H-MRS brain metabolites, [^{11}C]-PBR28 uptake, and the diffusion parameter FA in different brain regions of interest in a large cohort of ALS participants (n = 40).

Our data demonstrate that ^{1}H-MRS markers of gliosis (increased mI/Cr) and neuronal injury (decreased NAA/Cr) colocalize and are correlated with increased levels of the glial marker 18 kDa TSPO, measured by [^{11}C]-PBR28-PET, in the precentral gyri. There were no correlations between [^{11}C]-PBR28 uptake and these ^{1}H-MRS metabolite ratios in the brain stem, or in the control region of the precuneus. Levels of mI/Cr and NAA/Cr in the precentral gyri, are also correlated with upper motor

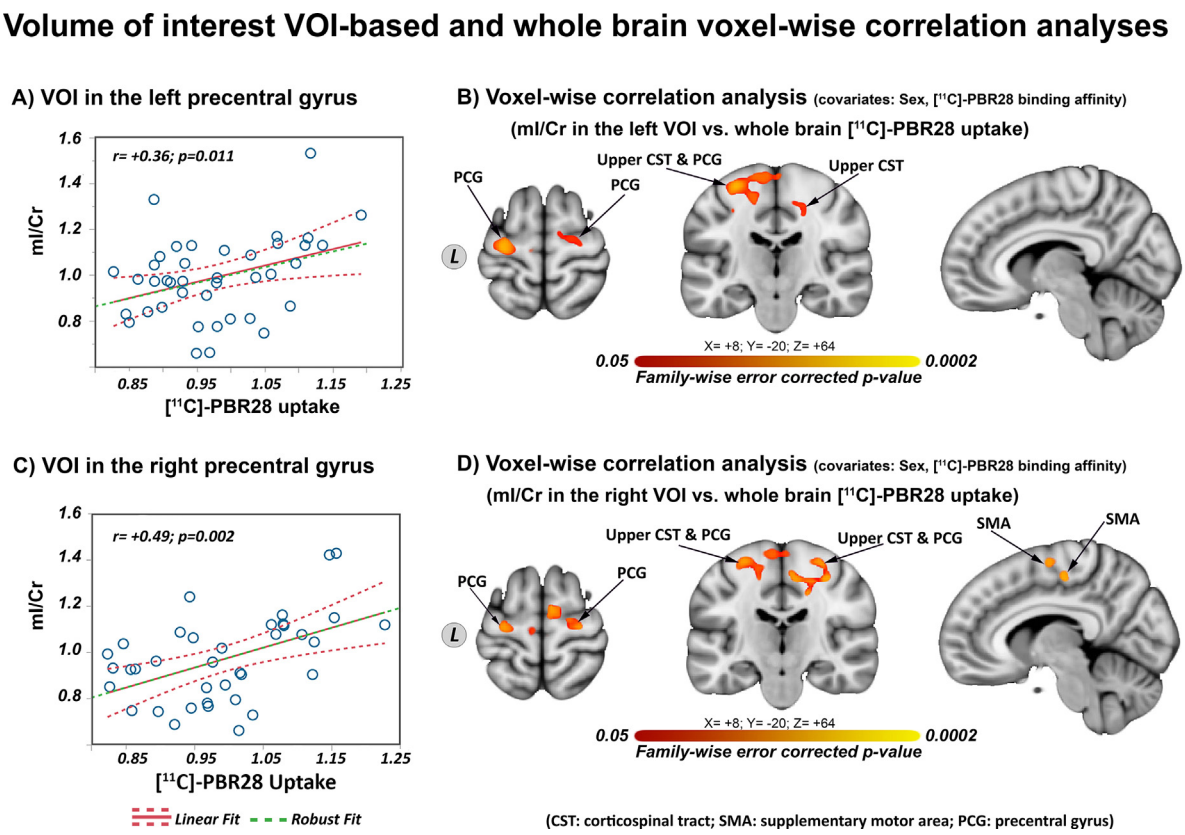

Fig. 1. Volume of interest (VOI)-based and voxel-wise correlation analyses between [^{11}C]-PBR28 uptake and mI/Cr.
Pearson correlation analyses between mI/Cr and [^{11}C]-PBR28 uptake in the left (A), and right (C) VOIs. The dashed red lines represent 95% confidence interval. The green dashed lines represent the robust fit of Pearson correlation based on Huber M-estimation. These correlations were confirmed by voxel-wise correlation analyses between [^{11}C]-PBR28 uptake in whole brain and mI/Cr measured in the left VOI (B) and right VOI (D). These whole brain voxel-wise correlations show positive correlations only in the precentral gyri. These analyses were carried out using non-parametric permutation inference (n = 5000 permutations), and the p values are family wise error corrected for multiple comparisons. The color bar of the voxel-wise correlation analyses (red to yellow) represents significant positive correlation. (For interpretation of the references to colour in this figure legend, the reader is referred to the web version of this article.)

neuron dysfunction measured by UMNB. In addition, lower functional status measured by ALSFRS-R is correlated with lower levels of NAA/Cr and higher levels of mI/Cr, mainly in the right precentral gyrus.

Myo-Inositol has been proposed as a glial marker (Brand et al., 1997), however, this role has been questioned (Rae, 2014). Previous studies in patients with ALS have shown that mI/Cr is elevated in the precentral gyri, which could be attributed to neuroinflammation in the brain of ALS patients (Kalra et al., 2006).

This present study provides very important, *in vivo,* evidence that links the findings of two different imaging modalities, namely, mI/Cr using ^{1}H-MRS and [^{11}C]-PBR28 uptake assessed by PET, that can independently assess gliosis and neuroinflammation in ALS patients. Interestingly, we found that mI/Cr and [^{11}C]-PBR28 uptake co-localize and are highly correlated only in the precentral gyri in ALS patients. On the other hand, there was no correlation or co-localization between [^{11}C]-PBR28 uptake and mI/Cr in the precuneus, a VOI that we had purposely included as negative control region as this area does not have a clear role in ALS pathophysiology. The findings of these correlations were confirmed by whole brain voxel-wise correlation analyses which showed an association between mI/Cr and [^{11}C]-PBR28 uptake, only in the precentral gyri. Overall, these data are in line with what we know from postmortem pathology about motor neuron degeneration in the precentral gyri and corticospinal tracts in people with ALS.

NAA is an established marker of neuronal integrity and a decrease in NAA relates to loss in neuronal density, neuronal dysfunction, and/or mitochondrial dysfunction (Moffett et al., 2007). Several neurodegenerative diseases including ALS are associated with decreased NAA levels in the relevant brain regions. Specifically, decreased NAA or NAA/Cr were reported in the motor cortices and the brain stem in ALS patients (Kenn et al., 2001; Kalra et al., 2006; Nelles et al., 2008; Sivak et al., 2010). Our data demonstrate that increased gliosis measured by [^{11}C]-PBR28 uptake in the precentral gyri co-localizes and correlates with neuronal injury/loss, measured by decreased NAA/Cr. Our study also demonstrates that both markers of neuronal integrity, NAA/Cr and FA, are highly correlated, and in line with the results of prior studies (Nelles et al., 2008; Liu et al., 2014; Stagg et al., 2013). One possible interpretation of these results is that we are seeing neuronal degeneration in the precentral gyri, measured by decreased NAA/Cr and FA, that is surrounded by activated microglial and reactive astrocytes, measured by increased [^{11}C]-PBR28 uptake and mI/Cr.

However, the causal relationship between these cellular events cannot be determined from this cross-sectional study. Longitudinal studies in early symptomatic or pre-symptomatic ALS gene carriers would be extremely valuable to elucidate the temporal relationship between neuronal degeneration and reactive gliosis.

There were no statistically significant correlations between [^{11}C]-PBR28 uptake and ^{1}H-MRS metabolites in the precuneus, which we selected as a control region because neither clinical phenotype nor postmortem pathology suggest the involvement of the precuneus in ALS. We believe that the absence of correlations in the precuneus reflects the fact that this region does not appear to exhibit increased neuroinflammation in people with ALS, as shown in previous TSPO imaging studies comparing ALS patients with healthy controls and employing first (Turner et al., 2004,2005), or second generation TSPO radioligands (Albrecht et al., 2016; Alshikho et al., 2018; Zurcher et al., 2015). TSPO is ubiquitously expressed at low levels in the central

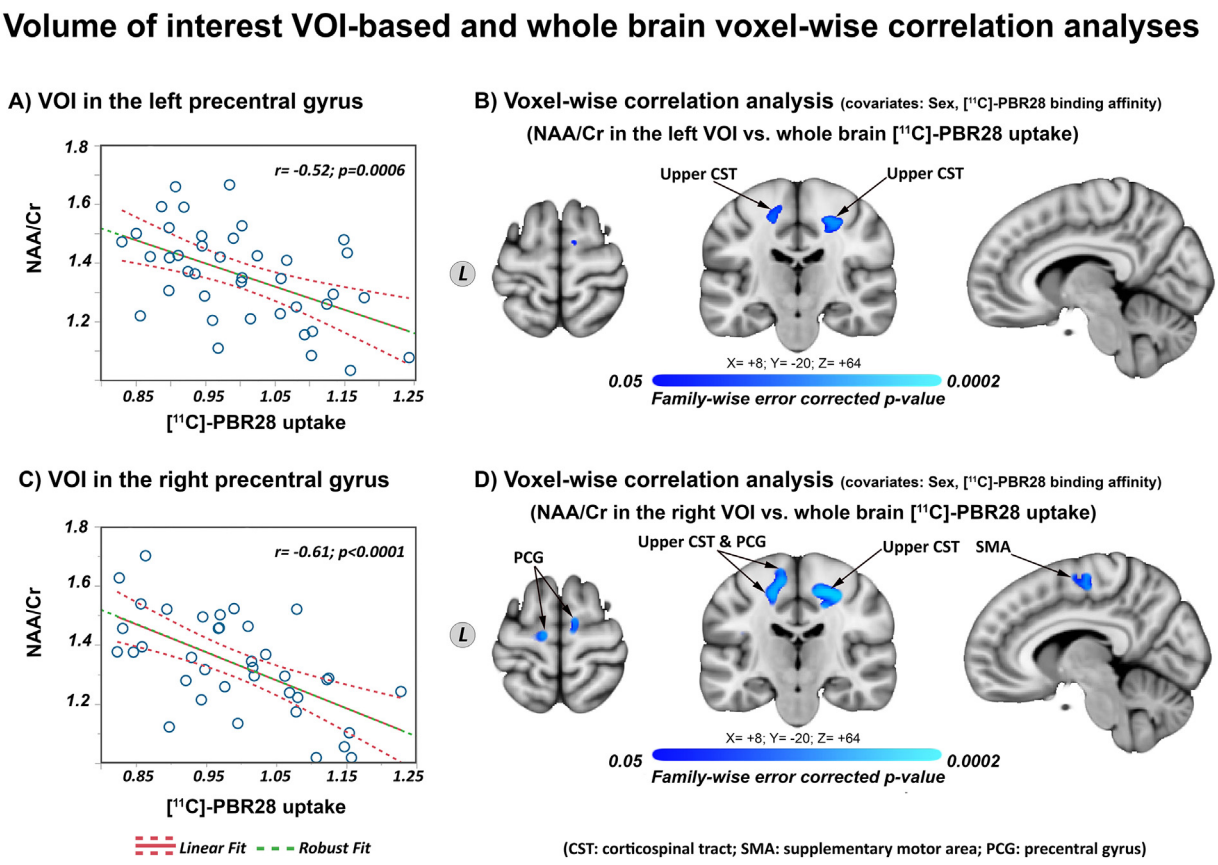

Fig. 2. Volume of interest (VOI)-based and voxel-wise correlation analyses between [^{11}C]-PBR28 uptake and NAA/Cr.
Pearson correlation analyses between NAA/Cr and [^{11}C]-PBR28 uptake in the left (A), and right (C) VOIs. The dashed red lines represent 95% confidence interval. The green dashed lines represent the robust fit of Pearson correlation based on Huber M-estimation. These correlations were confirmed by voxel-wise correlation analyses between [^{11}C]-PBR28 uptake in whole brain and NAA/Cr measured in the left VOI (B) and right VOI (D). These whole brain voxel-wise correlations show negative correlations only in the precentral gyri and the upper part of the corticospinal tracts. These analyses were carried out using non-parametric permutation inference (n = 5000 permutations), and the p values are family wise error corrected for multiple comparisons. The color bar of the voxel-wise correlation analyses (blue to cyan) represents significant negative correlation.

nervous system in healthy brain regions, and in these regions the low levels of TSPO expression only reflect the constitutive expression of this molecule, and are not indicative of neuroinflammatory processes, which manifest as an upregulation of TSPO expression measured by increased [^{11}C]-PBR28 uptake. The lack of correlation between [^{11}C]-PBR28 uptake and ^{1}H-MRS metabolites in brain regions not affected by the disease could be due to the low signal for [^{11}C]-PBR28 that is within the measurement noise. This hypothesis explains the concordance in the signal between the two putative neuroinflammatory markers (TSPO and mI/Cr) only in the specific motor cortex regions that are known to exhibit increased neuroinflammation in people with ALS.

It is also noteworthy that we also found no statistically significant correlations between [^{11}C]-PBR28 uptake and ^{1}H-MRS metabolites in the brain stem, a region that we hypothesized to be involved in ALS based on clinical and pathological grounds. There are few potential explanations for this lack of correlation. The brain stem region is a mix of upper motor neuron tracts and lower motor neuron nuclei for cranial nerves which may or may not be involved depending on each ALS patient's specific pathology. For instance, it is possible that the brain stem TSPO signal elevations might be present only in patients who have bulbar involvement, and the inclusion of only bulbar-onset or bulbar-affected patients, may allow to detect associations between [^{11}C]-PBR28 PET signal and ^{1}H-MRS metabolites in the brain stem. The brain stem is also a region in which the estimation of [^{11}C]-PBR28 PET is technically challenging, due to low signal-to-noise ratio (SNR), cardio-respiratory artifacts and other confounds notoriously affecting this region. Alternatively, it is possible that the molecular mechanisms mediating neuroinflammation in different regions of the brain might be different. Future larger studies will be needed to specifically address this question.

This study also validates the clinical relevance of several neuroimaging measures, including [^{11}C]-PBR28 uptake, mI/Cr, NAA/Cr and FA, as they are all correlated with increased upper motor neuron dysfunction measured by UMNB, and many were also found to be correlated with worse functional status measured by decreased ALSFRS-R. Few studies have explored the relationship between NAA and ALSFRS-R scores and have reported either no or relatively weak correlations (Stagg et al., 2013; Sivak et al., 2010; Han and Ma, 2010). Our previously published work has demonstrated correlations between [^{11}C]-PBR28 uptake, the fine motor sub-domain of the ALSFR-R scale and UMNB (Alshikho et al., 2018).

ALSFR-R is a clinical scale that predominantly reflects the loss of function due to muscle weakness, which is a consequence of lower rather than upper motor neuron degeneration. On the other hand, brain imaging studies represent changes to the upper motor neurons and their tracts, so a direct relationship between brain imaging parameters and ALS clinical functional status may not be intuitive. It is more logical that brain imaging parameters should correlate with measures of the upper motor neuron dysfunction, and represented by the strong correlations between UMNB and all the imaging measures which were evaluated in the precentral gyri. The weak correlations between ^{1}H-MRS metabolites in the precentral gyri and ALSFRS-R could represent a more complex relationship between the upper and lower motor neuron degeneration such as a dying back phenomenon.

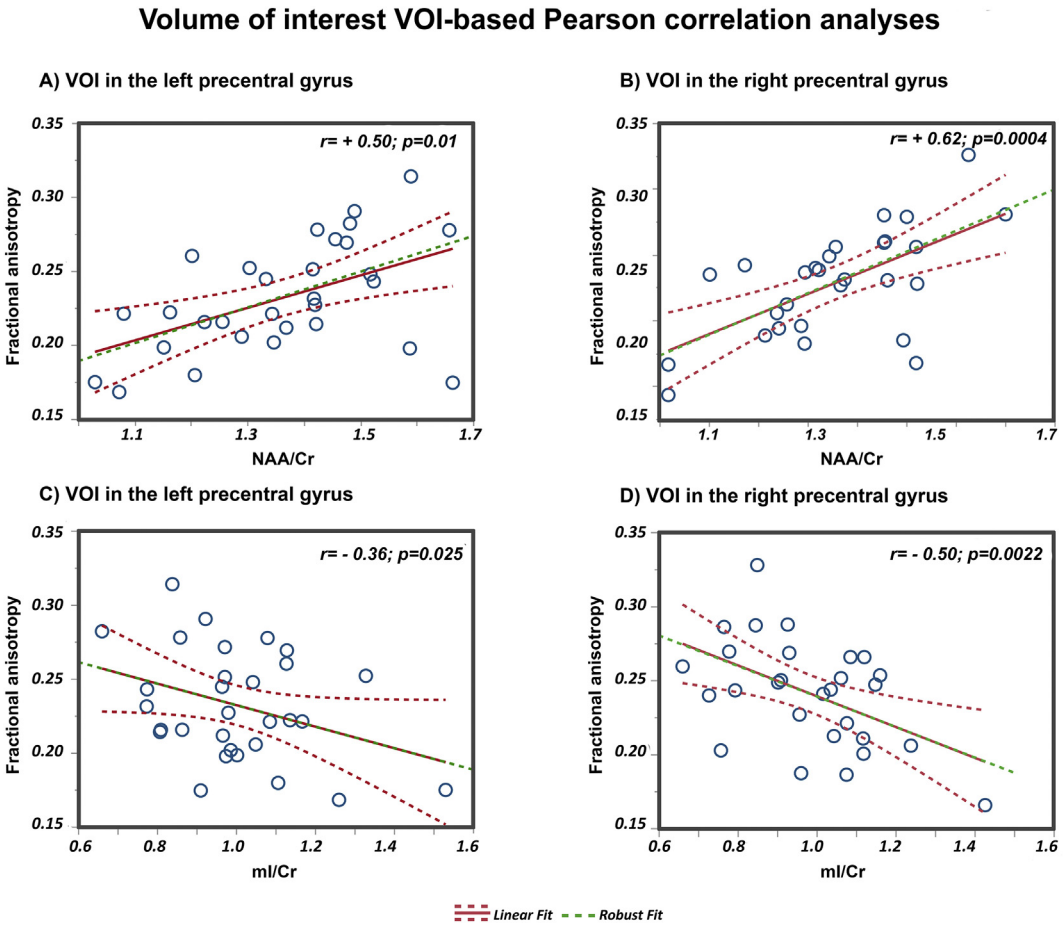

Fig. 3. Volume of interest (VOI)-based Pearson correlation analyses between FA, mI/Cr and NAA/Cr.
Pearson correlation analyses between FA, mI/Cr and NAA/Cr within VOI placed in the left precentral gyrus (A–C), and VOI in the right precentral gyrus (B–D). The dashed red lines represent 95% confidence interval. The green dashed lines represent the robust fit of correlation based on Huber M-estimation.

This study has several limitations. We would like to highlight that [^{11}C]-PBR28 and mI/Cr are non-specific markers of gliosis and glial activation, and cannot differentiate between different microglial phenotypes. Therefore, the biological implications of our results need to be interpreted with caution. Furthermore, no healthy controls were included in the study for comparisons. However, the major objective of this study was to determine the relationship between brain tissue metabolites measured by ^{1}H-MRS and glial activation assessed with [^{11}C]-PBR28 uptake in people with ALS. Another limitation of this current study is the lack of longitudinal data. Future longitudinal studies in early or pre-symptomatic ALS patients will help understand the temporal relationships of these molecular changes and clinical disease progression.

Combining multiple neuroimaging modalities is of great importance to unravel disease mechanisms in patients with ALS. Most of what we have learned about ALS disease mechanisms stems from postmortem pathology, SOD1 animal models, and different cell models. Although extremely valuable, these tools have major limitations. For example, the dynamics of postmortem cellular changes, and brain pathology after death miss valuable insights into the real picture of early neurodegeneration and does not allow for longitudinal tracking of evolving disease mechanisms. In addition, SOD1 animal models represent only 2% of human ALS (Rosen et al., 1993). Novel integrated molecular imaging technologies provide potential robust tools to study and accurately measure brain tissue alterations in the early stages of the disease.

The integrated PET-MR imaging tools implemented in this study could also serve as a molecular poof of the biological activity of experimental medications in the targeted disease tissue, which would potentially accelerate the pace of drug discovery in ALS. Using only clinical outcomes measures requires designing large, long, and expensive ALS clinical trials. With the absences of effective biomarkers to study ALS, there is an unmet need to develop molecular outcomes for efficient phase II clinical trials in ALS. Currently, there are four ongoing ALS clinical trials (NCT02525471, NCT02714036, NCT03127514, NCT02469896) that implement [^{11}C]-PBR28 and ^{1}H-MRS measurements as proofs of biological activity of these experimental treatments.

5. Conclusion

In conclusion, advanced molecular and structural imaging can be used to measure glial activation and neuronal degeneration in the precentral gyri in ALS patients. These integrated imaging technologies are poised to be invaluable tools to design efficient proof-of-mechanism ALS clinical trials.

Author contributions

Dr. Alshikho had full access to all the data in the study and takes responsibility for the integrity of the data and the accuracy of the data analysis. Dr. Ratai had access to ^{1}H-MRS data. Dr. Ratai and Dr. Alshikho are co–first authors and contributed equally to the study.

- Study concept and design: Dr. Ratai, Dr. Alshikho Dr. Zürcher, Dr. Loggia, Dr. Hooker, Dr. Atassi.
- Acquisition, analysis, or interpretation of data: All authors.
- Drafting of the manuscript: Dr. Ratai, Dr. Alshikho

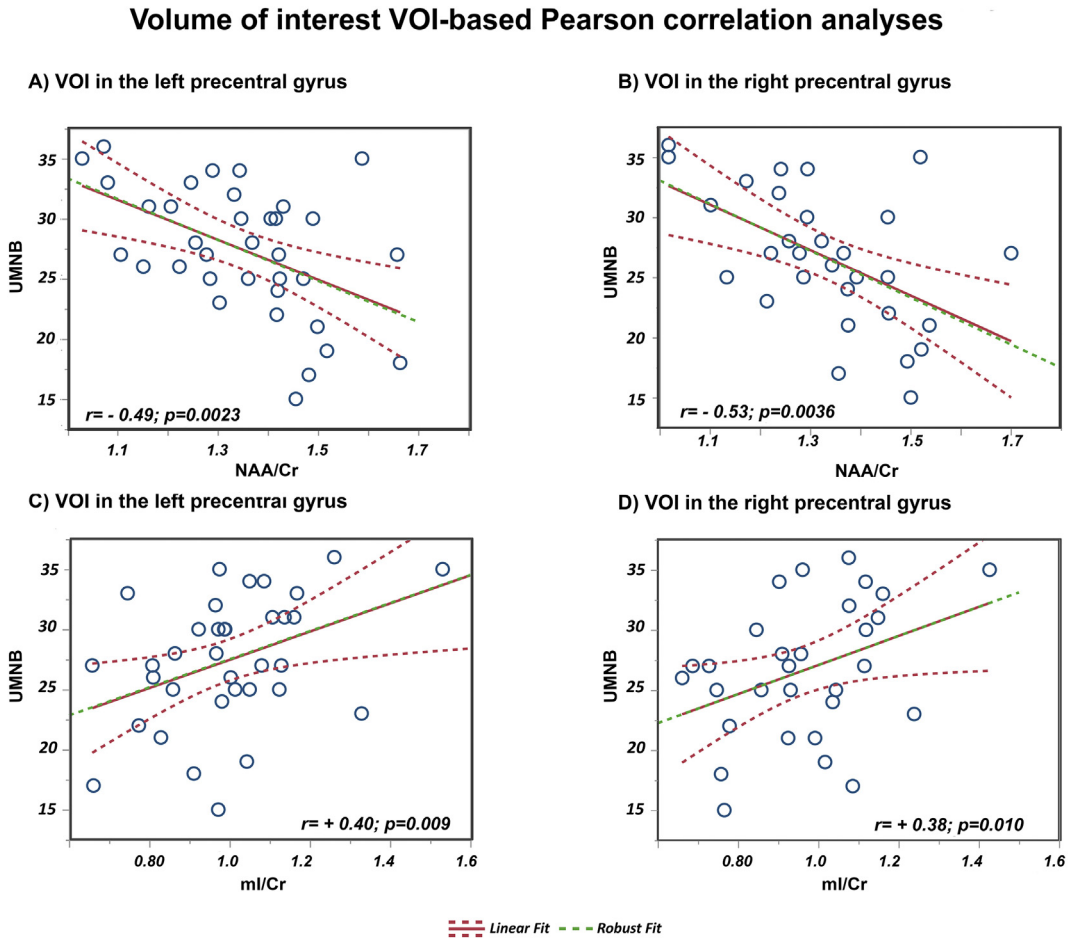

Fig. 4. Volume of interest (VOI)-based Pearson correlation analyses between UMNB, mI/Cr and NAA/Cr.
Pearson correlation analyses between upper motor neuron burden (UMNB), mI/Cr and NAA/Cr within VOI placed in the left precentral gyrus (A–C), and VOI in the right precentral gyrus (B–D). The dashed red lines represent 95% confidence interval. The green dashed lines represent the robust fit of correlation based on Huber M-estimation.

- Critical revision of the manuscript for important intellectual content: All authors
- Statistical analysis: Dr. Alshikho
- Obtained funding: Dr. Atassi
- Administrative, technical, or material support: Dr. Alshikho Dr. Zürcher, Dr. Loggia, Cebulla, Cernasov, Reynolds, Fish.
- Study supervision: Nazem Atassi and Jacob M. Hooker

Funding

This work was supported by Harvard NeuroDiscovery Center. The American Academy of Neurology, The Anne Young Fellowship award, The Spastic Paraplegia Foundation, and K23NS083715 from NINDS.

Author disclosure

- Eva-Maria Ratai is a member on the Advisory Board for BrainSpec, Inc. However, activity on the advisory board is not subject matter of this contribution.
- Mohamad J. Alshikho reports no disclosures
- Nicole R. Zürcher reports no disclosures
- Marco L. Loggia reports no disclosures
- Catherine L. Cebulla reports no disclosures
- Paul Michael Cernasov reports no disclosures
- Beverly Reynolds reports no disclosures
- Jennifer Fish reports no disclosures
- Raghav Seth reports no disclosures
- Suma Babu reports no disclosures
- Sabrina Paganoni has received research funding from Target ALS, the ALS association, ALS Finding a Cure, Amylyx, the Salah Foundation, The Harvard NeuroDiscovery Center, and the Spastic Paraplegia Foundation.
- Jacob M. Hooker reports no disclosures
- Nazem Atassi consulted for Biogen and Mitsubishi Tanabe

Supplementary data to this article can be found online at https://doi.org/10.1016/j.nicl.2018.08.007.

Acknowledgement

We thank our patients and their families for their kind contribution to research on amyotrophic lateral sclerosis. We also thank members of the Martinos Center for Biomedical Imaging radio pharmacy team and the NMR technicians Grae Arabasz, Shirley Hsu, and Regan Butterfield for their hard work, dedication, and support. This study was funded by Harvard Neuro-Discovery Center. The American Academy of Neurology, The Anne Young Fellowship award, The Spastic Paraplegia Foundation, and K23NS083715 from NINDS.

References

Albrecht, D.S., Granziera, C., Hooker, J.M., Loggia, M.L., 2016. In vivo imaging of human neuroinflammation. ACS Chem. Neurosci. 7, 470–483.
Alexianu, M.E., Kozovska, M., Appel, S.H., 2001. Immune reactivity in a mouse model of

familial ALS correlates with disease progression. Neurology 57, 1282–1289.
Alshikho, M.J., Zurcher, N.R., Loggia, M.L., Cernasov, P., Chonde, D.B., Izquierdo Garcia, D., Yasek, J.E., Akeju, O., Catana, C., Rosen, B.R., Cudkowicz, M.E., Hooker, J.M., Atassi, N., 2016. Glial activation colocalizes with structural abnormalities in amyotrophic lateral sclerosis. Neurology 87, 2554–2561.
Alshikho, M.J., Zurcher, N.R., Loggia, M.L., Cernasov, P., Reynolds, B., Pijanowski, O., Chonde, D.B., Izquierdo Garcia, D., Mainero, C., Catana, C., Chan, J., Babu, S., Paganoni, S., Hooker, J.M., Atassi, N., 2018. Integrated MRI and [(11) C]-PBR28 PET imaging in amyotrophic lateral sclerosis. Ann. Neurol. 83, 1186–1197.
Andersson, J.L.R., Sotiropoulos, S.N., 2016. An integrated approach to correction for off-resonance effects and subject movement in diffusion MR imaging. NeuroImage 125, 1063–1078.
Boillee, S., Yamanaka, K., Lobsiger, C.S., Copeland, N.G., Jenkins, N.A., Kassiotis, G., Kollias, G., Cleveland, D.W., 2006. Onset and progression in inherited ALS determined by motor neurons and microglia. Science 312, 1389–1392.
Brand, A., Leibfritz, D., Wolburg, H., Richter-Landsberg, C., 1997. Interactions of triethyltin-chloride (TET) with the energy metabolism of cultured rat brain astrocytes: studies by multinuclear magnetic resonance spectroscopy. Neurochem. Res. 22, 123–131.
Brettschneider, J., Toledo, J.B., VAN Deerlin, V.M., Elman, L., McCluskey, L., Lee, V.M., Trojanowski, J.Q., 2012. Microglial activation correlates with disease progression and upper motor neuron clinical symptoms in amyotrophic lateral sclerosis. PLoS One 7, e39216.
Briard, E., Zoghbi, S.S., Imaizumi, M., Gourley, J.P., Shetty, H.U., Hong, J., Cropley, V., Fujita, M., Innis, R.B., Pike, V.W., 2008. Synthesis and evaluation in monkey of two sensitive 11C-labeled aryloxyanilide ligands for imaging brain peripheral benzodiazepine receptors in vivo. J. Med. Chem. 51, 17–30.
Brooks, B.R., Miller, R.G., Swash, M., Munsat, T.L., World Federation of Neurology Research Group on Motor Neuron, D, 2000. El Escorial revisited: revised criteria for the diagnosis of amyotrophic lateral sclerosis. Amyotrop. Lateral Scler. Other Motor Neuron Disorders 1, 293–299.
Brown, A.K., Fujita, M., Fujimura, Y., Liow, J.S., Stabin, M., Ryu, Y.H., Imaizumi, M., Hong, J., Pike, V.W., Innis, R.B., 2007. Radiation dosimetry and biodistribution in monkey and man of 11C-PBR28: a PET radioligand to image inflammation. J. Nucl. Med. 48, 2072–2079.
Butovsky, O., Siddiqui, S., Gabriely, G., Lanser, A.J., Dake, B., Murugaiyan, G., Doykan, C.E., Wu, P.M., Gali, R.R., Iyer, L.K., Lawson, R., Berry, J., Krichevsky, A.M., Cudkowicz, M.E., Weiner, H.L., 2012. Modulating inflammatory monocytes with a unique microRNA gene signature ameliorates murine ALS. J. Clin. Invest. 122, 3063–3087.
Cady, J., Koval, E.D., Benitez, B.A., Zaidman, C., Jockel-Balsarotti, J., Allred, P., Baloh, R.H., Ravits, J., Simpson, E., Appel, S.H., Pestronk, A., Goate, A.M., Miller, T.M., Cruchaga, C., Harms, M.B., 2014. TREM2 variant p.R47H as a risk factor for sporadic amyotrophic lateral sclerosis. JAMA Neurol. 71, 449–453.
Catana, C., VAN DER Kouwe, A., Benner, T., Michel, C.J., Hamm, M., Fenchel, M., Fischl, B., Rosen, B., Schmand, M., Sorensen, A.G., 2010. Toward implementing an MRI-based PET attenuation-correction method for neurologic studies on the MR-PET brain prototype. J. Nucl. Med. 51, 1431–1438.
Cedarbaum, J.M., Stambler, N., Malta, E., Fuller, C., Hilt, D., Thurmond, B., Nakanishi, A., 1999. The ALSFRS-R: a revised ALS functional rating scale that incorporates assessments of respiratory function. BDNF ALS Study Group (Phase III). J. Neurol. Sci. 169, 13–21.
Guo, Q., Owen, D.R., Rabiner, E.A., Turkheimer, F.E., Gunn, R.N., 2014. A graphical method to compare the in vivo binding potential of PET radioligands in the absence of a reference region: application to [(1)(1)C]PBR28 and [(1)(8)F]PBR111 for TSPO imaging. J. Cereb. Blood Flow Metab. 34, 1162–1168.
Han, J., Ma, L., 2010. Study of the features of proton MR spectroscopy ((1)H-MRS) on amyotrophic lateral sclerosis. J. Magn. Reson. Imaging 31, 305–308.
Imaizumi, M., Kim, H.J., Zoghbi, S.S., Briard, E., Hong, J., Musachio, J.L., Ruetzler, C., Chuang, D.M., Pike, V.W., Innis, R.B., Fujita, M., 2007. PET imaging with [11C] PBR28 can localize and quantify upregulated peripheral benzodiazepine receptors associated with cerebral ischemia in rat. Neurosci. Lett. 411, 200–205.
Izquierdo-Garcia, D., Hansen, A.E., Förster, S., Benoit, D., Schachoff, S., Fürst, S., Chen, K.T., Chonde, D.B., Catana, C., 2014. An SPM8-based approach for attenuation correction combining segmentation and non-rigid template formation: application to simultaneous PET/MR brain imaging. J. Nucl. Med. 55, 1825–1830.
Jucaite, A., Svenningsson, P., Rinne, J.O., Cselenyi, Z., Varnas, K., Johnstrom, P., Amini, N., Kirjavainen, A., Helin, S., Minkwitz, M., Kugler, A.R., Posener, J.A., Budd, S., Halldin, C., Varrone, A., Farde, L., 2015. Effect of the myeloperoxidase inhibitor AZD3241 on microglia: a PET study in Parkinson's disease. Brain 138, 2687–2700.
Kalra, S., Hanstock, C.C., Martin, W.R., Allen, P.S., Johnston, W.S., 2006. Detection of cerebral degeneration in amyotrophic lateral sclerosis using high-field magnetic resonance spectroscopy. Arch. Neurol. 63, 1144–1148.
Kenn, W., Ochs, G., Pabst, T.A., Hahn, D., 2001. 1H spectroscopy in patients with amyotrophic lateral sclerosis. J. Neuroimaging 11, 293–297.
Kolb, A., Wehrl, H.F., Hofmann, M., Judenhofer, M.S., Eriksson, L., Ladebeck, R., Lichy, M.P., Byars, L., Michel, C., Schlemmer, H.P., Schmand, M., Claussen, C.D., Sossi, V., Pichler, B.J., 2012. Technical performance evaluation of a human brain PET/MRI system. Eur. Radiol. 22, 1776–1788.
Kreisl, W.C., Fujita, M., Fujimura, Y., Kimura, N., Jenko, K.J., Kannan, P., Hong, J., Morse, C.L., Zoghbi, S.S., Gladding, R.L., Jacobson, S., Oh, U., Pike, V. W. & Innis, R. B., 2010. Comparison of [(11)C]-(R)-PK 11195 and [(11)C]PBR28, two radioligands for translocator protein (18 kDa) in human and monkey: implications for positron emission tomographic imaging of this inflammation biomarker. NeuroImage 49, 2924–2932.
Lavisse, S., Guillermier, M., Herard, A.S., Petit, F., Delahaye, M., VAN Camp, N., Ben Haim, L., Lebon, V., Remy, P., Dolle, F., Delzescaux, T., Bonvento, G., Hantraye, P. & Escartin, C., 2012. Reactive astrocytes overexpress TSPO and are detected by TSPO positron emission tomography imaging. J. Neurosci. 32, 10809–10818.
Liu, X., Lai, Y., Wang, X., Hao, C., Chen, L., Zhou, Z., Yu, X. & Hong, N., 2014. A combined DTI and structural MRI study in medicated-naive chronic schizophrenia. Magn. Reson. Imaging 32, 1–8.
Moffett, J.R., Ross, B., Arun, P., Madhavarao, C.N., Namboodiri, A.M., 2007. N-Acetylaspartate in the CNS: from neurodiagnostics to neurobiology. Prog. Neurobiol. 81, 89–131.
Nelles, M., Block, W., Traber, F., Wullner, U., Schild, H.H., Urbach, H., 2008. Combined 3T diffusion tensor tractography and 1H-MR spectroscopy in motor neuron disease. AJNR Am. J. Neuroradiol. 29, 1708–1714.
Owen, D.R., Yeo, A.J., Gunn, R.N., Song, K., Wadsworth, G., Lewis, A., Rhodes, C., Pulford, D.J., Bennacef, I., Parker, C.A., Stjean, P.L., Cardon, L.R., Mooser, V.E., Matthews, P.M., Rabiner, E.A., Rubio, J.P., 2012. An 18-kDa translocator protein (TSPO) polymorphism explains differences in binding affinity of the PET radioligand PBR28. J. Cereb. Blood Flow Metab. 32, 1–5.
Paganoni, S., Alshikho, M.J., Zurcher, N.R., Cernasov, P., Babu, S., Loggia, M.L., Chan, J., Chonde, D.B., Garcia, D.I., Catana, C., Mainero, C., Rosen, B.R., Cudkowicz, M.E., Hooker, J.M., Atassi, N., 2018. Imaging of glia activation in people with primary lateral sclerosis. Neuroimage Clin. 17, 347–353.
Pohl, C., Block, W., Karitzky, J., Traber, F., Schmidt, S., Grothe, C., Lamerichs, R., Schild, H., Klockgether, T., 2001. Proton magnetic resonance spectroscopy of the motor cortex in 70 patients with amyotrophic lateral sclerosis. Arch. Neurol. 58, 729–735.
Rae, C.D., 2014. A guide to the metabolic pathways and function of metabolites observed in human brain 1H magnetic resonance spectra. Neurochem. Res. 39, 1–36.
Rosen, D.R., Siddique, T., Patterson, D., Figlewicz, D.A., Sapp, P., Hentati, A., Donaldson, D., Goto, J., O'Regan, J.P., Deng, H.X., et al., 1993. Mutations in Cu/Zn superoxide dismutase gene are associated with familial amyotrophic lateral sclerosis. Nature 362, 59–62.
Rupprecht, R., Papadopoulos, V., Rammes, G., Baghai, T.C., Fan, J., Akula, N., Groyer, G., Adams, D., Schumacher, M., 2010. Translocator protein (18 kDa) (TSPO) as a therapeutic target for neurological and psychiatric disorders. Nat. Rev. Drug Discov. 9, 971–988.
Sivak, S., Bittsansky, M., Kurca, E., Turcanova-Koprusakova, M., Grofik, M., Nosal, V., Polacek, H., Dobrota, D., 2010. Proton magnetic resonance spectroscopy in patients with early stages of amyotrophic lateral sclerosis. Neuroradiology 52, 1079–1085.
Smith, S.M., Nichols, T.E., 2009. Threshold-free cluster enhancement: addressing problems of smoothing, threshold dependence and localisation in cluster inference. NeuroImage 44, 83–98.
Sridharan, S., Lepelletier, F.X., Trigg, W., Banister, S., Reekie, T., Kassiou, M., Gerhard, A., Hinz, R., Boutin, H., 2017. Comparative evaluation of three TSPO PET radiotracers in a LPS-induced model of mild neuroinflammation in rats. Mol. Imaging Biol. 19, 77–89.
Stagg, C.J., Knight, S., Talbot, K., Jenkinson, M., Maudsley, A.A., Turner, M.R., 2013. Whole-brain magnetic resonance spectroscopic imaging measures are related to disability in ALS. Neurology 80, 610–615.
Turner, M.R., Cagnin, A., Turkheimer, F.E., Miller, C.C., Shaw, C.E., Brooks, D.J., Leigh, P.N., Banati, R.B., 2004. Evidence of widespread cerebral microglial activation in amyotrophic lateral sclerosis: an [11C](R)-PK11195 positron emission tomography study. Neurobiol. Dis. 15, 601–609.
Turner, M.R., Gerhard, A., Al-Chalabi, A., Shaw, C. E., Hughes, R. A., Banati, R. B., Brooks, D. J. & Leigh, P. N., 2005. Mills' and other isolated upper motor neurone syndromes: in vivo study with 11C-(R)-PK11195 PET. J. Neurol. Neurosurg. Psychiatry 76, 871–874.
Winkler, A.M., Ridgway, G.R., Webster, M.A., Smith, S.M., Nichols, T.E., 2014. Permutation inference for the general linear model. NeuroImage 92, 381–397.
Yeap, B.Y., Davidian, M., 2001. Robust two-stage estimation in hierarchical nonlinear models. Biometrics 57, 266–272.
Zurcher, N.R., Loggia, M.L., Lawson, R., Chonde, D.B., Izquierdo-Garcia, D., Yasek, J.E., Akeju, O., Catana, C., Rosen, B.R., Cudkowicz, M.E., Hooker, J.M., Atassi, N., 2015. Increased in vivo glial activation in patients with amyotrophic lateral sclerosis: assessed with [(11)C]-PBR28. NeuroImage Clin. 7, 409–414.